

Asymmetric terracing of lunar highland craters: Influence of pre-impact topography and structure

Ann W. Gifford and Ted A. Maxwell

Center for Earth and Planetary Studies, National Air and Space Museum, Smithsonian Institution,
Washington, DC 20560

Abstract—The effects of variable pre-impact topography and substrate on slumping and terrace formation have been studied on a group of 30 craters in the lunar highlands. These craters are characterized by a distinct upper slump block and are all situated on the rim of a larger, older crater or a degraded rim segment. Wide, isolated terraces occur where the rim of the younger crater coincides with a rim segment of the older crater. The craters are all located in Nectarian/pre-Nectarian highland units, and range in age from Imbrian to Copernican.

A proposed model for formation of slump blocks in these craters includes the existence of layers with different competence in an overturned rim of the pre-existing crater. Such layering could have resulted from overturning of more coherent layers during formation of the Nectarian and pre-Nectarian craters. A combination of material and topographic effects is therefore responsible for terrace formation. Similar terrain effects may be present on other planets and should be considered when interpreting crater statistics in relation to morphology.

INTRODUCTION

Slumping, terracing or wall failure is an important process in formation and modification of lunar craters. The process of slumping has been investigated by both geometrical (Cintala *et al.*, 1977) and theoretical models (Melosh, 1977; Melosh and McKinnon, 1979); however, these studies are dependent on morphologic constraints imposed by the geologic setting of the craters. Consequently, the study of slumped crater morphology is important for three reasons: 1) the process of crater wall failure is poorly understood although the characteristic morphology occurs in craters on the moon, Mars and Mercury; 2) the break in curve of lunar crater depth/diameter plots (Pike, 1974) may be related to wall slumping in craters with diameters greater than 15 km; and 3) the difference between diameter ranges of slumped craters in mare and highland regions may be related to substrate effects on crater morphology (Cintala *et al.*, 1977).

Analysis of crater wall failure based on the mechanics of near-surface materials suggests that large craters should collapse by both wall and floor failure resulting in vertical rise of the crater floor (Melosh, 1977). The break in slope of the depth/diameter curve for fresh lunar craters has been attributed to slumping of large craters (Gault *et al.*, 1975). However, Settle and Head (1979) have examined

slumping by means of a terrace restoration model which recreates the initial cavity based on present morphometric parameters. They have found that slump material alone cannot account for depth of craters larger than the inflection point in the depth/diameter plot. In a morphologic study of crater slumping, Cintala *et al.* (1977) divided wall failure models into "scallop" and "terraces," and interpreted the greater abundance of large scalloped craters in the lunar highlands to be the result of the more fragmental, less cohesive nature of the highland megaregolith. Although we agree with this two-fold division based on crater morphology, both substrate and pre-impact topography have affected a group of 30 asymmetrically terraced craters in the lunar highlands.

TERRACED CRATER MORPHOLOGY

The present study includes 30 craters located in the lunar farside highlands (Fig. 1, Table 1). They range in age from Imbrian to Copernican, and most are located in pre-Nectarian or Nectarian highlands. The craters are generally 15 to 40 km in diameter, but the majority cluster at about 27–30 km. These craters are all situated on the rims of larger, older craters, or degraded rim segments. The dominant mechanism of modification is extensive wall slumping and terrace formation, which takes the form of preferential slumping of wall material on one side of the crater. This distinct uppermost terrace-like ledge is much wider than any lower terraces or scallops within the crater (Fig. 2). These ledges vary from < 1 to ~ 10 km in width, corresponding to from 1 to 40% of the rimcrest diameter. The terraces are therefore substantially larger than normal terrace widths which average 2–4 km independent of crater size (Melosh, 1977).

These craters are also characterized by the relative lack of central peaks. Although 60% of fresh highland craters 30 km in diameter display central peaks, only 20% in this study have central peaks or possible remnants. Those central peaks that are present are generally composed of clusters of conical blocks or low mounds. Occasionally a low ridge near the center of the crater may be a remnant of a central peak; however, additional slumped material may have infilled the crater resulting in an uneven floor and possible masking of true central peaks.

Necho crater (5°S 123°E) (Fig. 2a) is the type example of a crater displaying asymmetric slumping in response to pre-existing topographic variations (Gifford *et al.*, 1979). The large terrace block on the western wall of the crater may have slumped as a result of reactivation of a subdued fracture oriented concentrically to the underlying large crater. Another crater (Plante) located within Keeler on the lunar farside (164°E 10.5°S) displays a very similar terrace block (Fig. 2b). Keeler is a younger crater than the crater underlying Necho with terrace ledges still apparent. The similar trend of the fresh upper scarp of Plante and the subdued terraces of Keeler is clear; this indicates reactivation of a concentric fracture by the subsequent impact. The excavation has caused this terrace to appear to be the age of the younger crater.

Large, isolated slump blocks are not confined to young craters. These terraces

Table 1. Locations, diameters, and ages of craters included in study.

Location of crater	Coordinates		Diameter (km)		Width of terrace (km)	Crater age	Age of impacted material
			Max	Min			
Plante	10.5S	164E	40	38	5-10	E	I
E of Keeler	11.5S	158E	32	29	5	E	I
E of Keeler	11S	154E	23	18	8	E	pN
Rim of Ventris	4.5S	158.5E	28	25	2	I	N
NE of Ventris	3.5S	160.5E	23	21	7	E	N
E of Ventris	2S	160E	19	17	2	E	N
E rim of Mendeleev	4N	145E	40	36	5	I	N
SE rim of Mendeleev	1N	143.5E	40	40	5	I	N
SW rim of Mendeleev	3N	139.5E	30	30	8	I	N
W rim of Mendeleev	5N	137E	23	21	3	I	N
S of Green	1N	133E	38	35	8	C	N
Rim of Vetchinkin	11N	134E	33	30	8	E	N
Rim of Vetchinkin	10N	132.5E	22	19	5	E	N
Necho	5S	123E	35	30	5	C	pN
Katchalsky	6.5S	116E	35	30	7	E	N/pN
NE of Saha	0.5S	108E	34	30	5	C	N/pN
Rim of Pasteur	9S	109E	40	40	4	E	pN
Rim of Kondratyuk	16S	115E	32	23	10	I	pN
Rim of Hilbert	16S	105E	27	25	13	I	N
Rim of Hilbert	15.5S	106E	17	13	5	I	N
Rim of Milne	35S	111E	38	30	4	C	N/pN
E of Jansky	9N	94E	19	16	4	E	N
Rim of Jansky	10N	91E	21	16	5	E	N
Rim of Neper	10N	84E	16	14	2	E	N
Rim of Kastner	7S	82E	14	11	3	I	pN
Thales	62N	50E	32	30	3	E	N
N of Strabo	65N	54E	30	28	4	E	N
Rim of Biela	54S	53E	26	24	5	I	pN
Rim of Hommel	56S	36E	34	30	4	E	N
SE of Hommel	58S	36E	30	27	3	E	N

have also formed on Imbrian-age craters (Fig. 3). Although subdued, the terrace ledges are similar when viewed in stereo. The craters are situated on the inner-rim walls of larger, old craters, and the slumping has occurred where two pre-existing rim walls overlap. Figure 3(b) shows two large degraded craters which share a rim, and two smaller superposed craters which have slumped in opposite directions, but in the direction of slope in each case. The smaller crater (white arrows) is only 13 km diameter, much smaller than craters in which terracing would normally occur (Cintala *et al.*, 1977). Consequently, we believe that the downhill slope and the older crater rim material have both encouraged slump formation in a crater which normally would not form such a large slump block.

The terraces of all craters studied coincide with the highest portion of the pre-existing topography. This occurs where the younger crater rim coincides with an

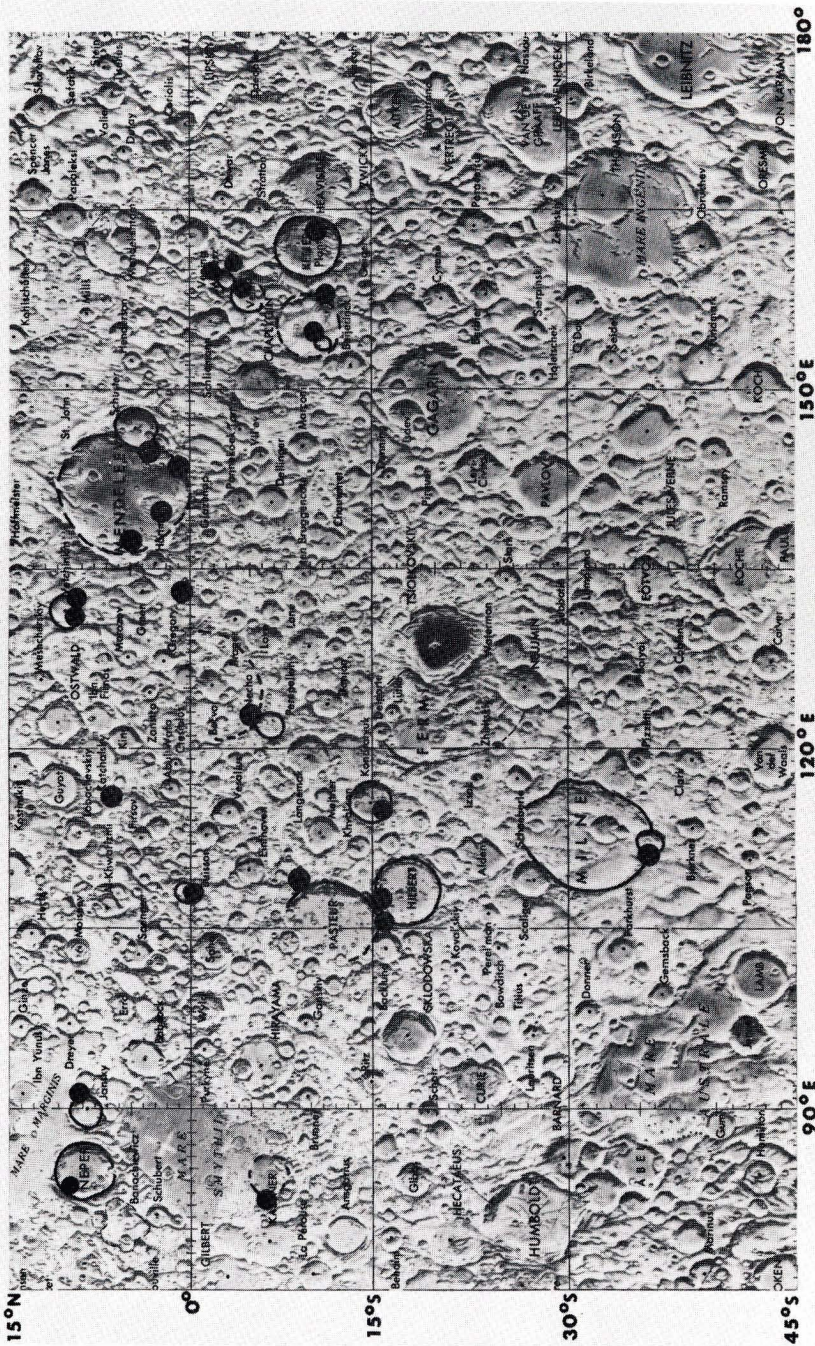


Fig. 1. Map showing location of 25 terraced craters included in study. All are located in the Nectarian/pre-Nectarian highlands of the lunar east limb and far side. Five additional craters are located in polar regions and are not shown on map. Map base is Lunar Chart (LPC-1) published by NASA.

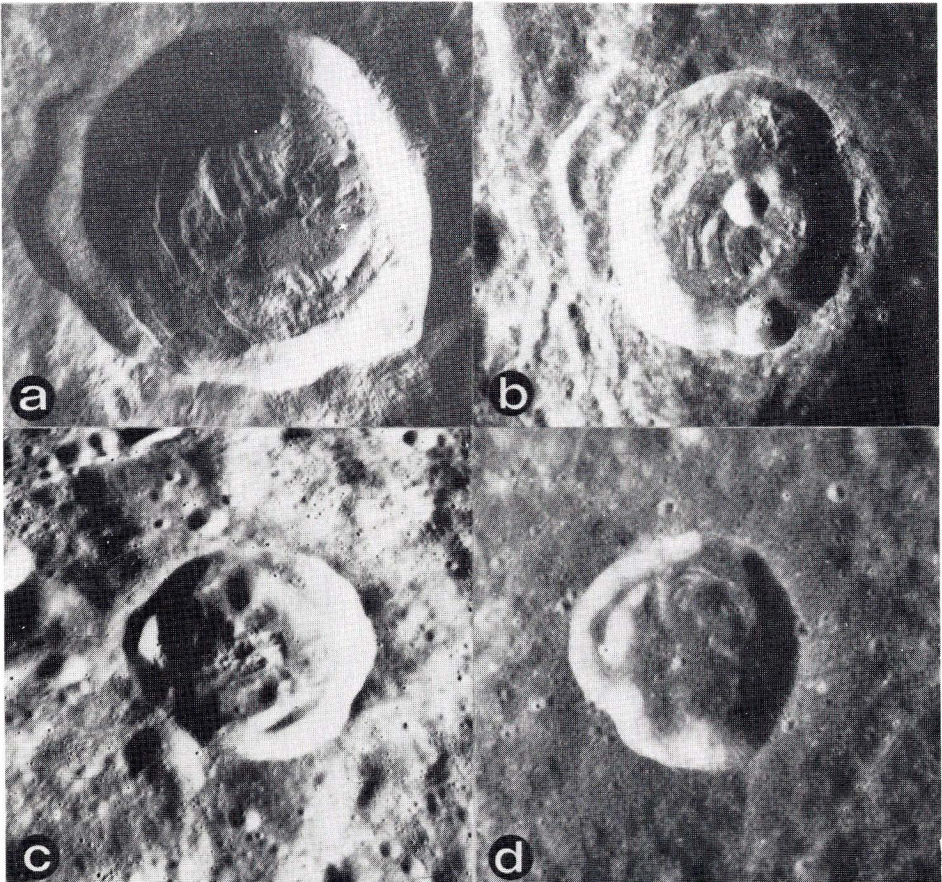


Fig. 2. (a) Necho crater (20 km dia.; 5°S 123°E). The prominent uppermost terrace coincides with the intersection of the rims of three underlying craters. (AS14-70-9671). (b) Plante crater (38 km dia.; 10°S 162°E) located at the eastern edge of Keeler crater (north towards the bottom). A portion of Plante's rim is superposed on the terraced wall of Keeler, forming a prominent ledge similar to Necho's uppermost terrace. The head scarp of this terrace is also concentric to Keeler, and is fresher than other terrace scarps associated with Keeler. (AS17-M-201) (c) 30-km crater at 11°N 134°E. This crater is located on the degraded rim of Vetchinkin northwest of Mendeleev. (AS16-M-1308) (d) 30-km crater at 11°S 158°E. This crater is on the rim of a very degraded 160-km crater west of Keeler. (AS17-M-352)

underlying crater rim segment. Large terraces apparently form in this manner under suitable topographic conditions even in cases where the predominant mode of wall failure is smaller-scale terracing. An example of this is Green crater (64 km dia., 4°N 133°E). The asymmetric location of these large slump blocks can therefore be related to topographic slope alone where substrate effects are not apparent.

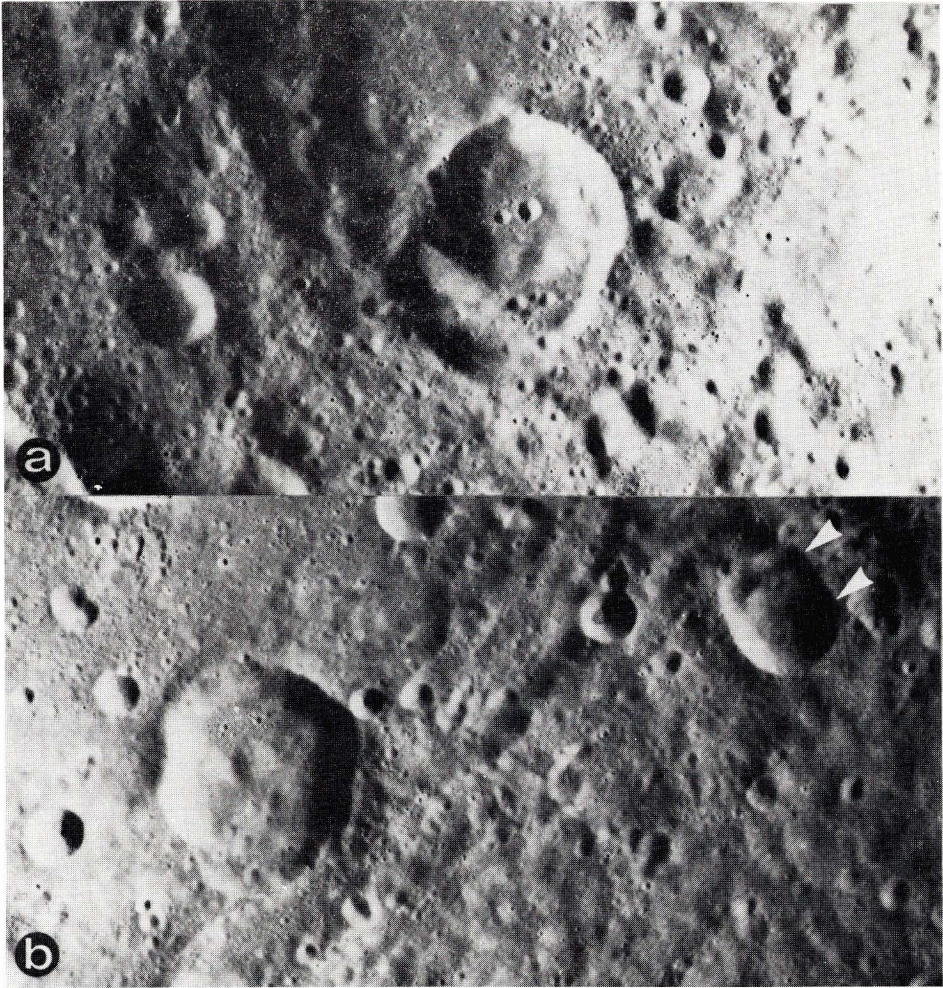


Fig. 3. (a) 28-km crater ($16^{\circ}\text{S } 115^{\circ}\text{E}$) located on the rim of Kondratyuk. (AS17-M-2809) (b) 27-km crater ($16^{\circ}\text{S } 105^{\circ}\text{E}$) and 13-km crater ($15.5^{\circ}\text{S } 106^{\circ}\text{E}$) located on a rim segment shared between the craters Pasteur and Hilbert. The trend of concentric scarps on the older rim segment is reflected by the terraces which have slumped into the smaller craters. (AS17-M-2815)

DISCUSSION

The group of lunar highland craters included in this study was defined on the basis of crater interior morphology. The diagnostic feature of this group is the occurrence of an asymmetric wall terrace located on the upper portion of the crater rim. These terraces are unusual because of their large width, especially

when compared with average crater terraces. The regional distribution of these craters is consistent with dominant control of the pre-impact geologic setting on final crater morphology. The absence of this class of craters near the Orientale basin is most likely the result of the significant ejecta deposition and modification of the lunar west side highlands accompanying the Orientale impact. Since several of the terraced craters are Eratosthenian or younger (Table 1), it is doubtful that Orientale ejecta deposition alone is responsible for their absence in this part of the moon. On a local scale, the geologic setting suggests that crater morphology was influenced by both topography and physical characteristics of the substrate.

The placement of the craters on large, older crater rims means that the impacts occurred on variably sloping ground. In the case of Necho (Gifford *et al.*, 1979) the western edge of the crater is superposed on an older crater rim, and the eastern half is at the base of the rim. The effect of pre-impact topography is shown by variations in rim crest elevation and interior morphology. In addition, the variation in rim crest elevation may also be related to deposits of impact melt surrounding the crater. Hawke and Head (1977) found that melt deposits occur predominantly opposite the maximum elevation of the crater rim. Stereoscopic examination of other craters in this group (where topographic data is lacking) reveals that irregular rim topography is common to all craters in this group. However, not all of these terraced craters occur on the interior rim of the older, pre-existing crater. Of the 30 craters included in this study, 9 occur on or adjacent to the exterior rim (Fig. 4). In all cases, however, the direction of slumping is away from the older rim crest.

There is no apparent relationship between terraced crater morphology and the age of the impacted material, although such a relation might provide a means of differentiating lithologic and mechanical attributes of the substrate from purely topographic effects. Instead, the distinctive terracing suggests a uniform response of the highlands materials despite probable lithologic differences. The fact that all of the craters in this group are located in the older (pre-Nectarian and Nectarian) highlands suggests that the blocky nature of the highlands material reinforces the tendency to slump more than a cohesive substrate (e.g., mare).

The extremely low percentage of central peaks in these craters may result from either lack of formation due to the mechanical properties of the substrate, or obliteration by slumping. The higher number of craters with central peaks in the mare versus the lunar highlands has been attributed to the more coherent nature of the mare lavas. According to crater statistics of Cintala *et al.* (1977), 90% of fresh mare craters in the 30 km size range have central peaks as opposed to only 60% of fresh highland craters. This difference has been interpreted to be the result of the more compressible highland megaregolith (Cintala *et al.*, 1977). In addition to non-formation of central peaks, their absence in these terraced craters may be due to destruction by wall failure. The pervasive nature of slumping in these craters may have acted to reduce or destroy central peaks. In Necho crater, for example, a probable central peak is offset from the center of the crater (by approximately 5 km) away from the rim terrace (Gifford *et al.*, 1979).

The formation of an upraised, overturned flap at the rim of an impact crater

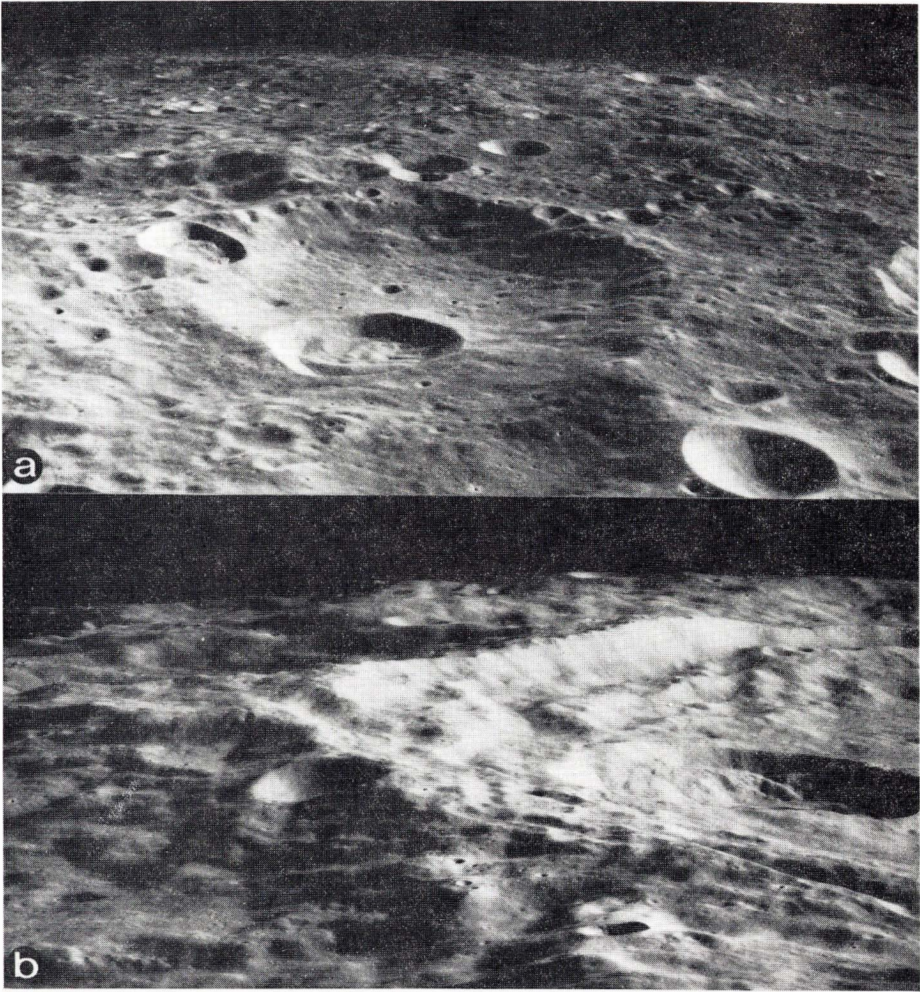


Fig. 4. (a) Oblique view of 25-km crater ($4.5^{\circ}\text{S } 158.5^{\circ}\text{E}$) on rim of Ventris (northwest of Keeler). (AS10-29-4178). (b) Oblique view of Plante (see Fig. 2(a)). (AS11-38-5570). These two pictures show the relation of the younger crater terraces to the underlying crater rim.

has been shown from field and experimental studies (Gault *et al.*, 1968). As shown in Fig. 5a, any difference in the competence of pre-existing layers should be present in the overturned flap. We suggest that if a more coherent layer was overturned in the pre-existing crater, then the substrate would favor slumping of a single large uppermost block in a superposed crater (Fig. 5b). As shown below, these conditions are consistent with models for the early evolution of the lunar highlands megaregolith.

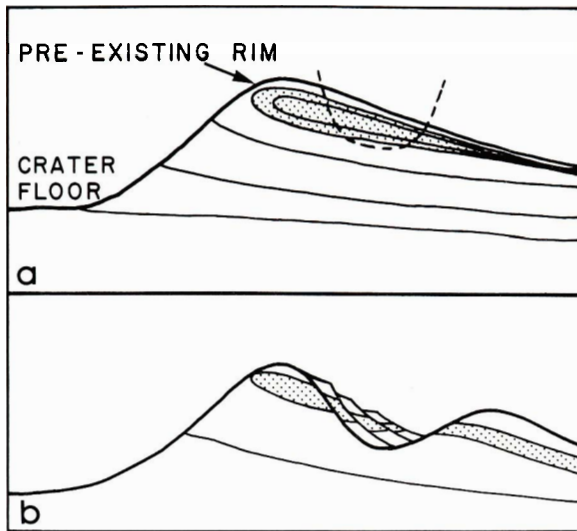


Fig. 5. Schematic view of one mechanism for asymmetric terrace formation. Younger crater forms on older crater rim where differences in layer coherency and topographic slope create conditions that favor isolated terrace formation.

Hartmann (1973) postulates a 2–3 km thick megaregolith layer in old highland surfaces underlain by a fractured crystalline layer. Quaide and Oberbeck (1968) and Head (1976) have suggested that this layer may account for changes in crater geometry once penetrated, specifically for the formation of concentric craters. However, earlier in lunar history, the megaregolith would have been thinner and more easily penetrated. Thus, a large crater would excavate both the megaregolith and the top of the fractured layer, resulting in an overturned flap that is more coherent than the surrounding megaregolith. Therefore any large crater in the highlands (especially older ones) would have the potential to sample more coherent layers. Consequently, it is likely that we are not seeing regional differences in highlands substrate, but rather the effect of older, larger craters penetrating the megaregolith. The concentric orientation of the headwalls of the terraces may also be aided by reactivation of fractures created by the older crater.

CONCLUSIONS

The distinction between this group of asymmetrically terraced craters and other highland craters that exhibit wall failure suggests that the local geologic setting has played the most important role in determining final crater morphology. The wide range in age of both the terraced craters and the impacted material suggests that despite probable lithologic differences in the highlands, pre-existing craters have created similar impact settings in certain areas of the lunar highlands. It is

most likely that slumping and terrace formation occurred during the terminal stages of the cratering event, when the local strength of the shocked material was at a minimum (McKinnon, 1978).

Formation of the single asymmetric terrace can be related to topography at the time of impact as well as earlier characteristics of the highlands regolith. We believe that the older craters (on which are superposed the terraced craters) have overturned rims made up of coherent bedrock, and were formed at a time when the highland megaregolith was thinner. Subsequent impact on or adjacent to crater rims was influenced by the pre-existing topography. In all cases, the single terrace that distinguishes this class of craters is oriented downslope with respect to the older crater. The occurrence of symmetrically terraced craters on Mars and Mercury (Wood *et al.*, 1978) suggests that similar terrain effects may be present on other planets. Fitting groups of morphologically distinct craters such as this into crater statistics may be a clue to documenting fine-scale controls on crater formation.

Acknowledgments—We thank F. El-Baz and C. A. Wood for helpful discussions at various stages of this investigation, and M. J. Cintala for constructive criticism of the manuscript.

Enlargements of Apollo photographs used in this study were provided by NSSDC. This study was supported by NASA Grant NSG-7188.

REFERENCES

- Cintala M. J., Wood C. A., and Head J. W. (1977) The effects of target characteristics on fresh crater morphology: Preliminary results for the moon and Mercury. *Proc. Lunar Sci. Conf. 8th*, p. 3409–3425.
- Gault D. E., Guest J. E., Murray J. B., Dzuris D., and Malin M. (1975) Some comparisons of impact craters on Mercury and the moon. *J. Geophys. Res.* **80**, 2444–2460.
- Gault D. E., Quaide W. L., and Oberbeck V. R. (1968) Impact cratering mechanics and structures. In *Shock Metamorphism of Natural Materials* (B. M. French and N. M. Short, eds.), p. 87–99. Mono, Baltimore.
- Gifford A. W., Maxwell T. A., and El-Baz F. (1979) Geology of the lunar farside crater Necho. *The Moon and the Planets*. In press.
- Hartmann W. K. (1973) Ancient lunar mega-regolith and subsurface structure. *Icarus* **18**, 634–636.
- Hawke B. R. and Head J. W. (1977) Impact melt on lunar crater rims. In *Impact and Explosion Cratering* (Roddy D. J., Pepin R. O., and Merrill R. B., eds.), p. 815–841. Pergamon, N.Y.
- Head J. W. (1976) The significance of substrate characteristics in determining morphology and morphology of lunar craters. *Proc. Lunar Sci. Conf. 7th*, p. 2913–2929.
- McKinnon W. B. (1978) An investigation into the role of plastic failure in crater modification. *Proc. Lunar Planet. Sci. Conf. 9th*, p. 3965–3973.
- Melosh H. J. (1977) Crater modification by gravity: A mechanical analysis of slumping. In *Impact and Explosion Cratering* (Roddy D. J., Pepin R. O., and Merrill R. B., eds.), p. 1245–1260, Pergamon, N.Y.
- Melosh H. J. and McKinnon W. B. (1979) Theoretical and experimental study of crater collapse (abstract). In *Lunar and Planetary Science X*, p. 830–832. Lunar and Planetary Institute, Houston.
- Pike R. J. (1974) Depth/diameter relations of fresh lunar craters: Revision from spacecraft data. *Geophys. Res. Lett.* **1**, 291–294.

- Quaide W. L. and Oberbeck V. R. (1968) Thickness determinations of the lunar surface layer from lunar impact craters. *J. Geophys. Res.* **73**, 5247–5270.
- Settle M. and Head J. W. (1979) The role of rim slumping in the modification of lunar impact craters. *J. Geophys. Res.* **84**, 3081–3096.
- Wood C. A., Head J. W., and Cintala M. J. (1978) Interior morphology of fresh martian craters: The effect of target characteristics. *Proc. Lunar Planet. Sci. Conf. 9th*, p. 3691–3709.